c_{d_i} (mm) as the diametrical clearance and a diameter D (m), the equivalent Damping number can be written as,

$$C_N = \frac{8 \times 10^9 n\mu\omega D(L_i/D)^3}{(c_{d_i}/D)^3} \quad (2)$$

The usefulness and application of the Damping Number (C_N) is explained in the following discussion. Consider the plot of growth factor vs. the retainer stiffness for, say, a clearance ratio of 3.25 mm/m, with a damper radius of 177.8 mm (7 in.) and a single land 76.2 mm (3 in.) wide.

To obtain the same stability for a different L/D ratio, the new clearance ratio can be calculated using the Damping Number. For example, if the same damper stiffness as the above configuration is desired in a damper with 2 lands, each 38.1 mm (1.5 in.) wide, the new clearance can be calculated as explained below. Let,

L_1, L_2 = land widths of the first and the second damper, respectively, (m)
n_1, n_2 = number of lands on the first and the second damper, respectively
c_{d1}, c_{d2} = diametrical clearance of the first and the second damper, (mm)
D_1, D_2 = diameter of the first and second the damper, (m)

Assuming the same effective viscosity and operating speed,

$$\frac{n_1 D_1 L_1^3}{c_{d_1}^3} = \frac{n_2 D_2 L_2^3}{c_{d_2}^3}$$

For the above example, $L_2 = L_1/2$ and $n_1 = 1$, $n_2 = 2$ and $D_1 = D_2$. Using these values we obtain the new equivalent clearance ratio to be 2.0 mm/m. This gives an example of the usefulness of the Damping Number. Hence, for a given rotor configuration, if one set of plots of stability vs. retainer stiffness (as in Fig. 1) are obtained, the Damping Number can be used to study the different configurations obtained by varying the length and number of lands, and the clearances, from the same plot. Figure 5 shows the plot of stability versus the retainer stiffness for the squeeze film damper with 2 lands each of width 38.1 mm (1.5 in.) and with an eccentricity ratio of 0.1. Comparing Figs. 1 and 5, it can be seen that the 3.25 mm/m clearance on the 76.2 mm (3 in.) wide damper corresponds to 2.0 mm/m on the 38.1 mm (1.5 in.) wide 2 land-damper. This confirms the calculation made by using the Damping Number.

The results generated for the stability of the rotor supported on a squeeze film damper with a single land of 76.2 mm (3 in.) wide, are applicable to other configurations of the damper, and need not be generated again. For the above example, where the new damper had 2 lands each of width 38.1 mm (1.5 in.), the lowest point on the plot in Fig. 1 would shift to 2 mm/m. The results could be correlated as follows. The lowest point on Fig. 2 would shift to the new clearance of 2.0 mm/m. In Fig. 4, the lowest point would again shift to the new clearance. Figure 5 would remain the same, for the clearance of 2.0 mm/m. This shows that the plots generated for one configuration could be used for other configurations of the squeeze film damper.

Conclusions

1. For a given rotor, the above design procedure can be adopted to obtain different configurations of the damper, and the stability analysis need be performed only for one configuration.
2. For a given retainer stiffness, the clearance of the damper can be optimized (see Fig. 2).
3. Increasing the operating eccentricity ratio decreases the stability of the rotor, for a given centered damper optimum clearance (see Figs. 3 and 4).
4. For a given rotor configuration, the changes in the parameters of the damper, viz., the land and clearance, can be determined by using the Damping Number (see Eq. (2)).
5. In general, the stability of the rotor can be improved by using a squeeze film damper, but care has to be taken in designing the damper, as it is very sensitive to changes in the clearances, operating eccentricity ratio, and nonlinear hardening retainer stiffness characteristics.

References

Kirk, R. G., 1980, "Stability and Damped Critical Speeds: How to Calculate and Interpret the Results," *CAGI Technical Digest,* Vol. 12, No. 2, pp. 375–383.

Mohan, S., and Hahn, E. J., 1974, "Design of Squeeze-film Damper Supports for Rigid Rotors," ASME *Journal of Engineering for Industry,* Vol. 96, No. 3, pp. 976–982.

Nelson, H. D., 1980, "A Finite Rotating Shaft Element Using Timoshenko Beam Theory," ASME *Journal of Mechanical Design,* Vol. 102, pp. 793–803.

Rabinowitz, M. D., and Hahn, E. J., 1977, "Stability of Squeeze-film Damper Supported Flexible Rotors," ASME *Journal of Engineering for Power,* Vol. 99, No. 4, pp. 552–558.

Rabinowitz, M. D., and Hahn, E. J., 1983, "Optimal Design of Squeeze Film Supports for Flexible Rotors," ASME *Journal of Engineering for Power,* Vol. 105, pp. 487–494.

Ramesh, K., and Kirk, R. G., 1992, "Subharmonic Resonance Stability Prediction for Turbomachinery with Active Magnetic Bearings," *Proceedings of the Third International Symposium on Magnetic Bearings,* pp. 113–122.

White, D. C., 1972, "The Dynamics of Rigid Rotor Supported on Squeeze Film Bearings," I. Mech. E., Conference on Vibration in Rotating Systems, pp. 213–229.

On the Modeling of a Thermomechanical Seizure

M. D. Pascovici,[1] M. M. Khonsari,[2] and J. Y. Jang[2]

Nomenclature

A = available area for convective heat transfer
A_f = friction area
c = specific heat
C = radial clearance
h = convective heat transfer coefficient
H = overall convective heat transfer
k = thermal conductivity
L = bearing length
M = system thermal capacity
R_b = bush inner radius
R_{bo} = bush outer radius
R_s = shaft radius
t = time
T = temperature
T_0 = reference temperature
δ_s = shaft radial expansion
α_s = coefficient of thermal expansion
β = temperature-viscosity coefficient
θ = dimensionless temperature
κ = material thermal diffusivity
μ = lubricant viscosity
μ_0 = initial lubricant viscosity
ρ = density

[1] Department of Mechanical Engineering, Polytechnical University of Bucharest, Bucharest, Romania 79590.

[2] Department of Mechanical Engineering, University of Pittsburgh, Pittsburgh, PA 15261.

Contributed by the Technology Division of THE AMERICAN SOCIETY OF MECHANICAL ENGINEERS. Manuscript received by the Technology Division March 11, 1994; revised manuscript received February 15, 1995. Associate Technical Editor: M. J. Braun.

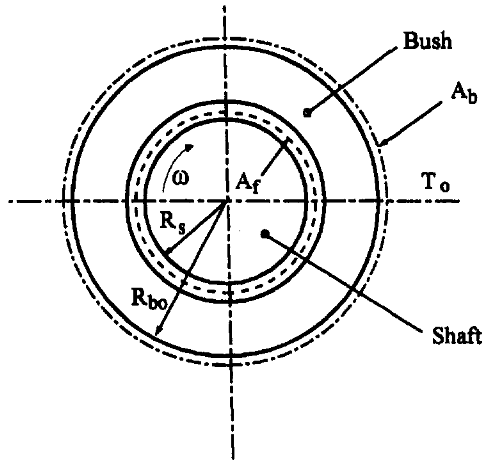

Fig. 1 (*a*) Infinitely long bearing

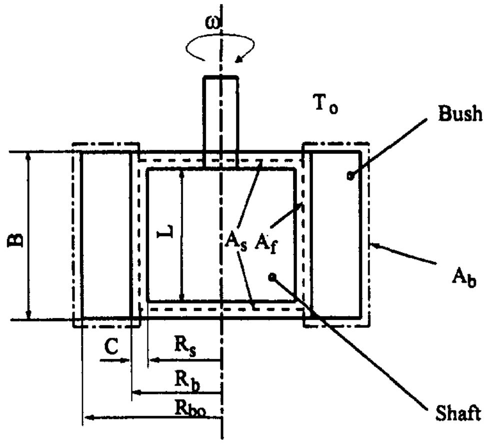

Fig. 1 (*b*) Submerged system

Fig. 1 Geometry of the model for lumped-system analysis

τ = dimensionless time
ω = shaft rotational speed

Subscripts

b = bushing
s = shaft

Introduction

Bearing seizure is a form of instability that drives a system to rapidly lose its operating clearance, thus leading to a catastrophic failure. Most susceptible to this type of failure mode are bearings with inadequate lubrication which, particularly during the start-up period, experience an excessive amount of frictional heat generation as a result of (nearly) dry rubbing. Analyses pertaining to this form of seizure have been the subject of a number of research papers. See for example, Dufrane and Kannel (1989), Khonsari and Kim (1989), and Hazlett and Khonsari (1992a, b) who studied the nature of the shaft expansion as it encroaches on the sleeve in a journal bearing.

This paper deals with the seizure of a fully lubricated journal bearing. The underlying nature of both dry and lubricated seizure is thermomechanical expansion. However, the existence of fluid considerably complicates the analytical formulation of this transient behavior.

To gain insight into the seizure phenomenon, a simple model is developed that allows one to establish a relationship between the key parameters that influence the seizure time in a hydrodynamic bearing. For this purpose, the journal bearing system is represented by two concentric cylinders with the inner cylinder rotating at a constant speed while the outer cylinder remains stationary. The clearance space is uniform and fully lubricated with a Newtonian fluid. This system is an idealized one. It essentially represents a Petroff's-type journal bearing and is akin to a rotational viscometer. We seek a closed-form, analytical expression for time of seizure in this bearing configuration with particular interest in developing an appropriate conditions(s) whereby seizure can be avoided.

Table 1 Bearing specifications and input data

Bearing dimensions	
R_{bo}	0.04 m
R	0.025 m
L	0.05 m
C	0.000025 m
Oil properties	
k	0.13 W/m K
ρ	860 kg/m^3
c	2000 J/kg K
μ_0	0.03 Pa.s
T_0	20°C
Shaft properties	
k	54 W/m K
κ	0.0000152 m^2/s
α	0.00002 m/m K
Bush properties	
k	49.84 W/m K
κ	0.000017 m^2/s
Convective heat transfer coefficient	
h_b	20 W/m^2 K
h_s	20 W/m^2 K

Energy Balance

Performing an energy balance for the entire system based on a lumped-system analysis yields the following equation.

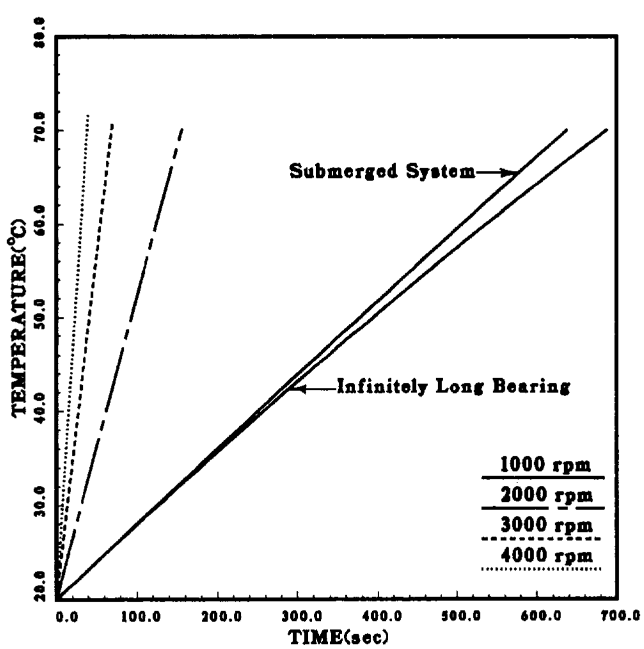

Fig. 2 Temperature as a function of time

$$M \frac{dT}{dt} = A_f \mu \frac{R_s^2 \omega^2}{C - \delta_s} - AH(T - T_0), \tag{1}$$

where

$$M = \rho_s c_s V_s + \rho_b c_b V_b$$

$$A = A_s + A_b$$

$$H = \frac{A_s h_s + A_b h_b}{A_s + A_b}.$$

The parameter δ_s represents the shaft thermal expansion in the radial direction in accordance to $\delta_s = \alpha_s R_s (T - T_0)$, where α_s is the shaft thermal expansion. The left-hand side of equation (1) represents the energy stored in the system as time proceeds. The first term on the right-hand side is the viscous dissipation term—derived based on the Petroff's formulation of frictional torque, and the last term stands for energy loss by convection. The parameter T_0 represents the ambient temperature and the initial temperature of the system.

With the nonlinear viscosity-temperature relationship of $\mu = \mu_0 e^{-\beta(T-T_0)}$, the above equation reduces to:

$$\frac{d\theta}{d\tau} = \xi_1 \frac{e^{-\bar{\beta}\theta}}{1 - \xi_3 \theta} - \xi_2 \theta, \tag{2}$$

where

$$\theta = \frac{T - T_0}{T_0}; \quad \tau = \omega t; \quad \bar{\beta} = T_0 \beta$$

$$\xi_1 = \frac{A_f R_s^2 \mu_0 \omega}{M T_0 C}; \quad \xi_2 = \frac{AH}{M\omega}; \quad \xi_3 = \frac{\alpha_s R_s T_0}{C}.$$

This equation does not easily lend itself to a closed-form analytical solution. Therefore, for simplicity, we shall make the assumption that the lubricant viscosity varies as a function of film thickness in accordance to the equation:

$$\mu = \mu_0 \frac{C - \delta_s}{C}. \tag{3}$$

The relationship shown in Eq. (3), first put forward by Tipei, has been shown to yield good general agreement with experimental results (cf. Tipei, 1960).

Using the above relationship, Eq. (1) becomes

$$\frac{d\theta}{d\tau} = \xi_1 - \xi_2 \theta. \tag{4}$$

The solution to Eq. (4) is:

$$\theta = \frac{\xi_1}{\xi_2}(1 - e^{-\xi_2 \tau}). \tag{5}$$

The limiting temperature at the onset of seizure when the clearance is completely vanished occurs when $\theta^* = 1/\xi_3$ and corresponding seizure time is:

$$\tau^* = \frac{1}{\xi_2} \ln \left(\frac{\xi_1 \xi_3}{\xi_1 \xi_3 - \xi_2} \right). \tag{6}$$

Seizure can be avoided if the steady state solution $\theta_\infty = \xi_1/\xi_2$ is kept below the limiting temperature θ^*, i.e., when

$$\frac{\xi_1}{\xi_2} < \frac{1}{\xi_3}. \tag{7}$$

Substituting expressions for ξ_1 through ξ_3 yields the following general expression which will be referred to as the "no-seizure" condition:

$$\Gamma \equiv \frac{\mu_0 \alpha_s}{H} \frac{A_f}{A} R_s^3 \left(\frac{\omega}{C} \right)^2 < 1. \tag{8}$$

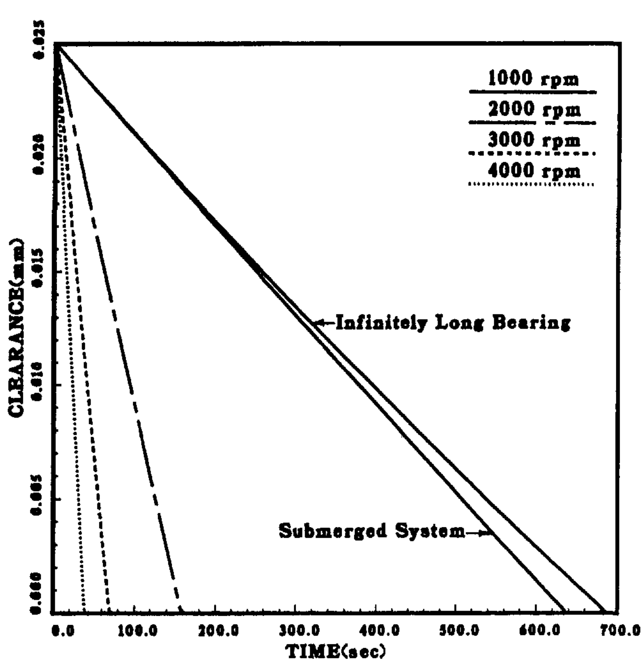

Fig. 3 Clearance variation as a function of time

Special Cases

I. Infinitely Long Bearing. Let us consider the case of an infinitely long bearing (Fig. 1(a)) where we have:

$$A = 2\pi R_{bo} \cdot 1 \quad \text{and} \quad H = h_b$$

$$A_f = 2\pi R_s \cdot 1 \tag{9}$$

The no-seizure condition of Eq. (8) now reads:

$$\frac{\mu_0 \alpha_s}{h_b} \frac{R_s^4}{R_{bo}} \left(\frac{\omega}{C} \right)^2 < 1. \tag{10}$$

II. Submerged System. If the system (journal and sleeve) is submerged, referring to Fig. 1(b), we have:

$$h_s \gg h_b; \quad A \approx A_s = 2\pi R_s^2 \quad \text{and} \quad H \approx h_s$$

$$A_f = 2\pi R_s L \tag{11}$$

The no-seizure condition in this case becomes:

$$\frac{\mu_0 \alpha_s L R_s^2}{h_s} \left(\frac{\omega}{C} \right)^2 < 1. \tag{12}$$

Equations (10) and (12) provide appropriate relationships between the bearing parameters that must be satisfied in order to avoid seizure. The physical interpretation of these seizure conditions is clear: to avoid seizure, one must choose a shorter bearing length (for the submerged system) and a shaft material with a small thermal expansion coefficient. A low lubricant viscosity improves the seizure time due to less viscous dissipation. Similarly, for improvement of the thermal characteristic of the bearing, a high convective heat transfer coefficient is helpful. The most important parameters affecting the thermally induced seizure are the shaft speed and R/C ratio. If the speed and the shaft diameter are fixed by design constraints, then enlarging the clearance may be considered as a possible solution. However, this option must be carefully analyzed at the design stage since whirl instabilities can set in when the clearance is large.

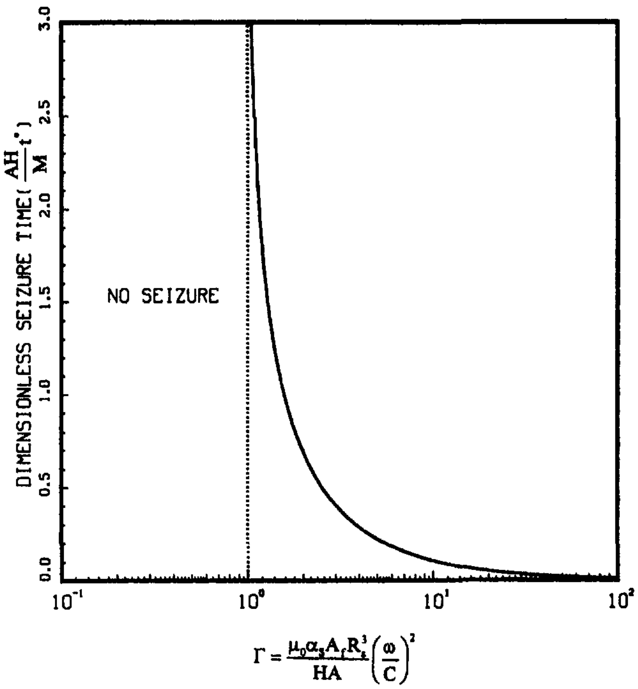

Fig. 4 Seizure map

Discussion

To gain further insight into the seizure problem and also to illustrate the utility of the equations derived, let us consider a journal bearing system with the specifications shown in Table 1. The thermal response of this bearing for several rotational speeds is depicted in Fig. 2 with the corresponding clearance variations as a function of time shown in Fig. 3. The difference between the infinitely long bearing and the submerged system is mainly confined to lower rotational speeds (e.g., 1000 rpm). At higher speeds the results are nearly identical. Both models predict that at a relatively large shaft speed of 3000 rpm, the temperature of the system rapidly rises from 20°C to 70°C, causing a complete loss in clearance within roughly 1 minute of operation. At lower shaft speeds such as 1000 rpm, the onset of seizure is considerably delayed (roughly 10 minutes for the submerged case). It is to be noted, however, that at low speed the onset of seizure becomes more dependent upon the model and the convective heat transfer coefficient assumed. Finally, a general seizure map is presented in Fig. 4 using the definition of Γ in Eq. (8) and a dimensionless seizure time $(AH/M)t^*$, where $t^* = \tau^*/\omega$. Using Fig. 4 one can easily estimate the onset of seizure. Note that in accordance to criterion of Eq. (8), seizure is suppressed for values of less $\Gamma < 1$.

Concluding Remarks

A study of thermally induced seizure in hydrodynamic bearings requires a detailed transient thermohydrodynamic analysis which must take into account the thermoelastic nature of the surfaces. Such analyses require complicated numerical solutions. To gain insight into the phenomenon of seizure in hydrodynamic journal bearings, a model is developed based on the lumped-system analysis which lends itself to a closed-form analytical solution. Such an analysis is, of course, best suited for a system whose Biot number is small. The formulation provides a criterion for avoiding seizure that can be easily checked at the design stage. A general seizure map for estimating the onset of seizure is also provided.

References

Dufrane, K. F., and Kannel, J. W., 1989, "Thermally Induced Seizure of Journal Bearings," ASME Journal of Tribology, Vol. 111, pp. 288–292.

Hazlett, T. L., and Khonsari, M. M., 1992a, "Finite Element Model of Journal Bearings Undergoing Rapid Thermally Induced Seizure," *Tribology International,* Vol. 25, pp. 177–182.

Hazlett, T. L., and Khonsari, M. M., 1992b, "Thermoelastic Behavior of Journal Bearings Undergoing Seizure," *Tribology International,* Vol. 25, pp. 183–187.

Khonsari, M. M., and Kim, H. J., 1989, "On Thermally Induced Seizure in Journal Bearings," ASME Journal of Tribology, Vol. 111, pp. 661–667.

Tipei, N., 1960, *Theory of Lubrication,* Stanford University Press, Stanford CA.